




Article

Optimizing Mineralization of Bioprinted Bone Utilizing Type-2 Fuzzy Systems

Ashkan Sedigh ¹, Mohammad-R. Akbarzadeh-T. ² and Ryan E. Tomlinson ^{1,*}¹ Department of Orthopaedic Surgery, Thomas Jefferson University, Philadelphia, PA 19107, USA² Department of Electrical Engineering, Center of Excellence on Soft Computing and Intelligent Information Processing, Ferdowsi University of Mashhad, Mashhad 9177948944, Iran

* Correspondence: ryan.tomlinson@jefferson.edu

Abstract: Bioprinting is an emerging tissue engineering method used to generate cell-laden scaffolds with high spatial resolution. Bioprinting parameters, such as pressure, nozzle size, and speed, highly influence the quality of the bioprinted construct. Moreover, cell suspension density and other critical biological parameters directly impact the biological function. Therefore, an approximation model that can be used to find the optimal bioprinting parameter settings for bioprinted constructs is highly desirable. Here, we propose a type-2 fuzzy model to handle the uncertainty and imprecision in the approximation model. Specifically, we focus on the biological parameters, such as the culture period, that can be used to maximize the output value (mineralization volume 21.8 mm³ with the same culture period of 21 days). We have also implemented a type-1 fuzzy model and compared the results with the proposed type-2 fuzzy model using two levels of uncertainty. We hypothesize that the type-2 fuzzy model may be preferred in biological systems due to the inherent vagueness and imprecision of the input data. Our numerical results confirm this hypothesis. More specifically, the type-2 fuzzy model with a high uncertainty boundary (30%) is superior to type-1 and type-2 fuzzy systems with low uncertainty boundaries in the overall output approximation error for bone bioprinting inputs.



Citation: Sedigh, A.; Akbarzadeh-T., M.-R.; Tomlinson, R.E. Optimizing Mineralization of Bioprinted Bone Utilizing Type-2 Fuzzy Systems.

Biophysica **2022**, *2*, 400–411.

<https://doi.org/10.3390/biophysica2040035>

<https://doi.org/10.3390/biophysica2040035>

Academic Editor: Leo Massari

Received: 1 September 2022

Accepted: 18 October 2022

Published: 28 October 2022

Publisher's Note: MDPI stays neutral with regard to jurisdictional claims in published maps and institutional affiliations.



Copyright: © 2022 by the authors. Licensee MDPI, Basel, Switzerland. This article is an open access article distributed under the terms and conditions of the Creative Commons Attribution (CC BY) license (<https://creativecommons.org/licenses/by/4.0/>).

Keywords: bioprinting; fuzzy systems; type-2 fuzzy logic; optimization; approximation

1. Introduction

Additive manufacturing is a process by which three-dimensional objects are generated by material deposition in sequential layers [1,2]. Bioprinting is an emerging field of additive manufacturing in which bioactive scaffolds can be quickly generated by depositing layers of cell-laden biocompatible materials, such as collagen or other hydrogels. After specifying the exact geometry of the construct, a G-code containing the extrusion path and parameters is generated to direct fabrication by one of several commercially available desktop bioprinters. Indeed, the ability to place cells in biologically relevant scaffold materials with a high spatial resolution has made bioprinting a popular fabrication method for tissue engineering [3,4].

In addition to the specific geometry of the bioprinted construct, the parameters used to perform the bioprinting procedure itself will have significant effects on the final properties of the model. Therefore, it is essential to fully characterize and optimize the bioprinting parameters (e.g., print speed or bioink viscosity) necessary to reach the desired outputs, such as high cell viability, appropriate cell function, and necessary mechanical properties [5]. For example, increasing the nozzle size on the bioprinter decreases the shear stress placed on the biomaterial during extrusion, which results in increased cell viability and reduced print resolution [6]. Therefore, determining the optimal print parameters is imperative for success in bioprinting. As a result, several studies have been performed in the field of bioprinting optimization, such as optimization of a solid model for 3D bioprinting, bioink optimization, and bioprinting parameter selection [7,8].

Determining printability using universal parameters is challenging due to the variability of customized bioinks. Moreover, this complexity is increased in bioinks with multiple

extracellular matrix (ECM) components that affect the rheological properties and can result in non-linear relationships between input and output parameters [9,10]. The results from our previous study suggest that the computational approach is useful for optimizing printing parameters and will improve reproducibility across diverse bioinks as well as provide an objective characterization of bioprinting precision for newly formulated bioinks. In this paper, we investigate the computational optimization of the ECM components in bioprinting.

Nonetheless, there is a significant degree of imprecision and uncertainty inherent in bioprinting optimization. A potential approach to handling this issue, which arises from normal biological variation, is through the implementation of approximation systems based on computational methods [11]. In recent years, systems biology has become a critical multidisciplinary research area between computer science and biology. Studies in this field aim to develop computational models of biological processes, which requires both a robust dynamic model and well a large dataset of experimental results.

Developing a dynamic model is challenging and requires well-characterized control parameters to approximate laboratory experiments' outcomes. Nonetheless, recent studies have observed that computational optimization algorithms can effectively approximate output parameters using either a deterministic or stochastic biological model. A partial list of the approaches employed to this end includes meta-heuristic, evolutionary, global optimization, genetic programming, simulated annealing, simplex, ant-colony, fuzzy genetic hybrid system, and multi-objective optimization. In-silico models have helped reproducibility and quality in the in-vitro experiments significantly in tissue engineering [12,13].

Here, we have developed a quantitative model of a biological system using the fuzzy system approach, which is a potential solution for overcoming uncertainty in an experimental dataset. In fact, previous studies have shown that the accuracy of a fuzzy system approach is the same as the deterministic mathematical approach (ordinary differential equations) for the same kinetic dataset. Moreover, fuzzy systems can be utilized to find the qualitative system response when a quantitative dataset is not available [14]. Theoretical fuzzy models have been used in decision making systems to predict biomechanical properties as stress/strain of a bone structure in a biological process [15].

Fuzzy logic is an extended model of standard logic. In standard logic, truth values can only be either completely false or completely true (with degrees of truth equal to 0 or 1, respectively), whereas, in fuzzy logic, values can have a degree of truth between 0 and 1. This generalization provides a mathematical framework to move from discrete to continuous values. In other words, in contrast to sets in classical logic, a fuzzy set is a set without a crisp boundary. For instance, if the reference set X is a Universe of discourse for elements x , the fuzzy set A is defined as:

$$A = \{ (x, \mu_A(x)) | x \in X \}$$

where $\mu_A(x)$ is called the Membership Function (MF) for the fuzzy set A . The MF maps each element of the Universe set X to a grade between 0 and 1, i.e., a membership of 0 means that the associated element is not included, whereas a membership of 1 means an element is fully included.

A fuzzy rule-based system is a modeling framework that uses the above fuzzy set theory along with a set of "if-then" rules where the antecedents and consequents are fuzzy logic propositions. This rule-based fuzzy system is used for modelling the inputs and their relationships with the output variables. A type-1 Fuzzy System (T1 FS) is a framework consisting of weighted rules, membership functions, and a fuzzy inference system. This system takes the crisp data (fuzzy singletons) or fuzzy inputs and generates fuzzy outputs based on the given if-then rules. A method of defuzzification is then used to extract a crisp value inferred from the fuzzy model.

A type-2 fuzzy system (T2 FS) is also similar to its type-1 counterpart, but includes a type-reducer and defuzzifier, which generate a type-1 fuzzy set output and then a crisp number, respectively. T2 FS have been widely applied to a variety of problems where

handling uncertainty is critical, including decision making, function approximation, and data preprocessing [16–18]. One example is a model with noisy and uncertain training data: in this model, uncertainty exists in the antecedent and consequents. The level of uncertainty and information regarding it can be used in mathematical modeling of antecedents and consequents. Moreover, non-quantitative data is often disseminated using words that convey an indistinct level of certainty [19]. T2 FS has the capability to grade these linguistic representations into membership functions, which shows a more robust algorithm rather than T1 FS in inferencing input data. However, the computational cost of T2 FS is higher than the T1 FS [19].

The main objective of this study is to implement fuzzy systems to model and find the optimal bioprinting parameters. We hypothesize that the implementation of a T2 FS would reduce the error in the output in biological systems with inherent uncertainty in both the inputs and outputs.

To directly test this hypothesis, in Section 2 we implement type-1 and type-2 fuzzy logic systems with the experimental dataset. We then evaluate and compare the performance of each for use in the approximation of bioprinting output in Section 3. Section 4 describes how fuzzy systems can optimize the bioprinting and biological parameters.

Type-2 Fuzzy System

The concept of a Type-2 fuzzy set is an extension of the ordinary type-1 fuzzy set, as originally introduced by Zadeh [20]. In contrast to a T1 FS, Type-2 fuzzy sets have grades of membership that are themselves fuzzy both in primary and secondary memberships. A primary membership is the same as a type-1 membership that maps each element to a grade between 0 and 1. Relative to each primary membership, there is a secondary membership (a grade between 0 and 1) that describes the uncertainty in defining the primary membership using a fuzzy set construct.

The general diagram of a T2 Mamdani fuzzy logic system is shown in Figure 1, including the fuzzification, fuzzy inference, Karnik–Mendel type reduction, and defuzzification steps. Considering the crisp inputs (n inputs) and one output:

$$x_1 \in X_1, \dots, x_n \in X_n \text{ and } y \in Y,$$

the k -th ($k = 1, \dots, K$) rule in Mamdani T2 FS is expressed as:

$$R^k : \text{if } x_1 \text{ is } \tilde{F}_1^k \text{ and } \dots \text{ and } x_n \text{ is } \tilde{F}_n^k, \text{ then } y \text{ is } \tilde{G}^k$$

where \tilde{F}_1^k and \tilde{G}^k are type-2 fuzzy sets. In this system, rules represent the fuzzy relations between multiple dimensional input space $X \triangleq X_1 \times \dots \times X_n$ and output space Y . The definitions below are paraphrased from the Mendel and Liang article in T2 FS [21]:

Definition 1. (Footprint of Uncertainty of a Type-2 Membership Function): Uncertainty in the region between the upper and lower boundaries of a Type-2 membership function is called the footprint of uncertainty. It is the union of all primary membership grades.

Definition 2. (Upper and Lower MFs): A type-1 fuzzy upper and lower boundary MFs for the Footprint of Uncertainty, and (FOU) of an interval type-2 MF. The upper and lower bounds of the region are the maximum and minimum membership grades of FOU (Figure 1-fuzzification [21]).

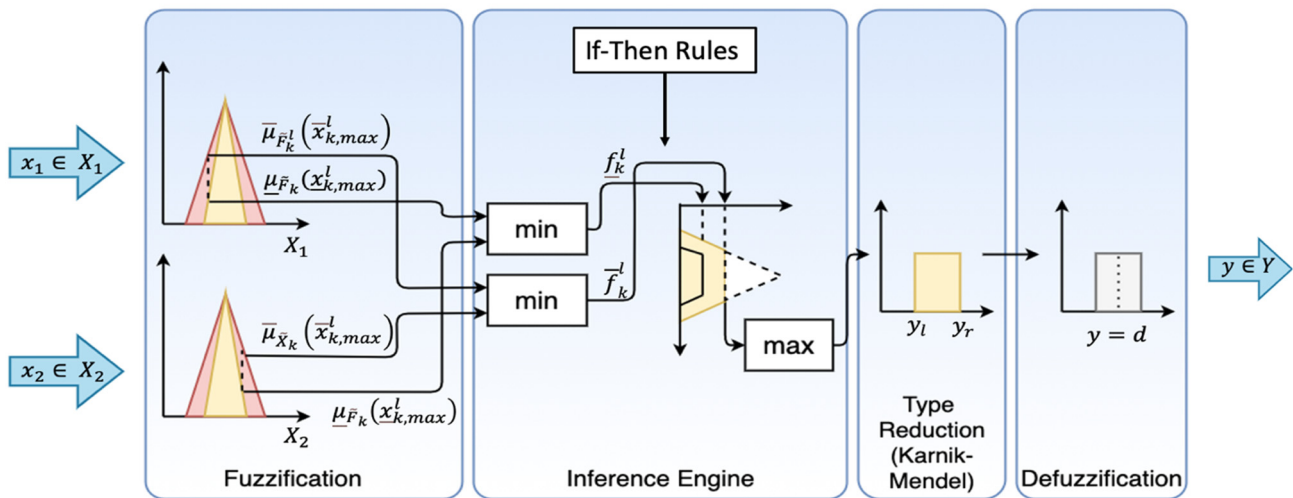


Figure 1. Type-2 Fuzzy Logic Algorithm and Study Design. General overview and different features of the Type-2 Fuzzy system including fuzzification, rules, inference engine, type reduction, and defuzzification. The T2 FS structure includes the *min* and *max* operations as fuzzification and inference engine process.

The over and under bars show the upper and lower MFs, respectively. The membership function of \tilde{F}_1^k is represented as:

$$\mu_{\tilde{F}_1^k}(x_k) = \int_{\omega^l \in [\underline{\mu}_{\tilde{F}_1^k}(x_k), \overline{\mu}_{\tilde{F}_1^k}(x_k)]} 1/\omega^l \tag{1}$$

The upper and lower boundaries on a Gaussian primary function with an uncertain standard deviation is represented below. In this representation, the Gaussian primary MF has a fixed mean m_k^l and an uncertain standard deviation $\sigma_k^l \in [\sigma_{k1}^l, \sigma_{k2}^l]$:

$$\mu_k^l(x_k) = \exp\left[-\frac{1}{2} \left(\frac{x_k - m_k^l}{\sigma_k^l}\right)^2\right] \tag{2}$$

where

$$k \in (1, \dots, \text{number of antecedents})$$

$$l \in (1, \dots, \text{number of rules})$$

The upper and lower MF of $\mu_k^l(x_k)$ are:

$$\overline{\mu}_k^l(x_k) = \mathcal{N}(m_k^l, \sigma_{k2}^l; x_k) \quad \text{upper MF}$$

$$\underline{\mu}_k^l(x_k) = \mathcal{N}(m_k^l, \sigma_{k1}^l; x_k) \quad \text{lower MF}$$

In the interval T2 non-singleton fuzzy system with type-2 fuzzification and minimum or product t-norm, the output fuzzy set is represented as:

$$\mu_{\tilde{B}}(y) = \int_{b \in [[\underline{f}^1 * \underline{\mu}_{\tilde{G}1}(y)] \vee \dots \vee [\underline{f}^N * \underline{\mu}_{\tilde{G}N}(y)], [\overline{f}^1 * \overline{\mu}_{\tilde{G}1}(y)] \vee \dots \vee [\overline{f}^N * \overline{\mu}_{\tilde{G}N}(y)]]} \frac{1}{b} \tag{3}$$

In (3), \underline{f} and \overline{f} are the result of the input and antecedent operations (Figure 1-Inference engine), based on the value of x_k , in which the supremum occurs as $\underline{x}_{k,max}^l$ and $\overline{x}_{k,max}^l$:

$$\overline{f}_k^l = \overline{\mu}_{\tilde{X}_k}(\overline{x}_{k,max}^l) * \overline{\mu}_{\tilde{F}_k^l}(\overline{x}_{k,max}^l) \tag{4}$$

$$\underline{f}_k^l = \underline{\mu}_{\tilde{x}_k} \left(x_{k,max}^l \right) \star \underline{\mu}_{\tilde{f}_k} \left(x_{k,max}^l \right) \quad (5)$$

In the algorithm above, we follow the following steps to obtain the crisp output: (1) fuzzification, (2) fuzzy inference, (3) type-reduction, and (4) defuzzification. The result of crisp input and antecedents is an interval type-1 fuzzy set, defined by the lower and upper MF \underline{f} and \overline{f} , respectively. Referring to (3), the fired output value, which is the combined output consequent set $\mu_{\tilde{B}}(y)$, is computed. The type-2 fuzzy system is computationally intensive to implement. A potential solution is a type-reduction method, as proposed by Kendrick and Mendel for the type-1 defuzzification method for reducing the type-2 to type-1 fuzzy system [21].

Various forms of type-reduction algorithms are proposed as centroid and center-of-sets [22]. In our method, we have used the center-of-set type-reduction method (Figure 1-type reduction):

$$y_l = \frac{\sum_{i=1}^M f_l^i y_l^i}{\sum_{i=1}^M f_l^i} \text{ and } y_r = \frac{\sum_{i=1}^M f_r^i y_r^i}{\sum_{i=1}^M f_r^i}, \quad (6)$$

where the maximum and minimum value of y are y_r and y_l , respectively; y_r and y_l depend only on a mixture of f and \overline{f} values, because $f^i \in F^i = [f, \overline{f}]$. Due to y being an interval non-convex set, we defuzzify it by using the average of y_r and y_l (Figure 1-defuzzification).

$$f(x) = \frac{y_r + y_l}{2} = d, \quad (7)$$

where d is the defuzzified output in the above formula.

2. Methods

2.1. Fuzzy Inference Engine

The first step to develop this approximation model is to make a fuzzy inference system, such as the Mamdani or Sugeno systems. For this study, we chose the Mamdani inference engine due to the intuitive interpretable nature of its rule-based inferencing.

The main difference between Mamdani-type and Sugeno-type Fuzzy Inference System (FIS) is the method of how the output result is obtained. In Mamdani FIS, the crisp result is obtained through defuzzification of the rules. However, Sugeno FIS uses a weighted average of the rules to compute the crisp output. Moreover, Mamdani FIS can be applied to both "Multiple Input, Single Output" (MISO) and "Multiple Input, Multiple Output" (MIMO) systems, which is advantageous for biologic systems that frequently have multiple outputs. It is important to note that Sugeno-type systems can be used for MISO systems.

2.2. Membership Function Variables and Parameterization

We obtained optimization data for the variables in our model from a previously published experimental study [23]. As shown in Figure 2, the bioprinting approximation system has two inputs, which are the number of cells (millions per milliliter) and the culture period (days), and one output variable, which is the mineralized volume of the bioprinted construct (mm³). The prior knowledge defines the membership function values and If-Then rules in the T2 fuzzy model as shown in Figure 2.

The mineralized volume of the bioprinted bone was calculated based on registered microCT scans using previously established methods [24]. Here, microCT imaging was performed after 7, 14, 21, 28, 35, and 42 days in culture [23].

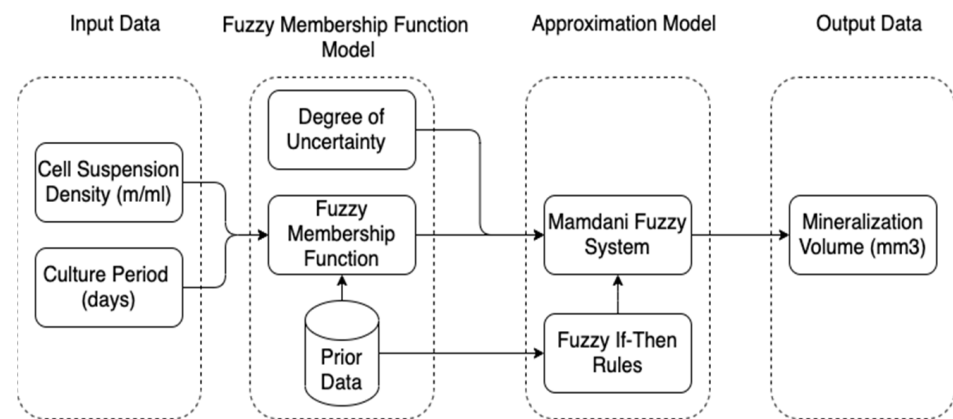


Figure 2. Schematic of our study design optimization technique, with two inputs (cell suspension density and culture period) and one output (mineralization volume).

Next, the membership functions (MFs) were defined. MFs are distributed evenly by dividing the full input data range by the number of MFs, which is the input labels shown in Table 1 and Figure 3. The membership function is a 2D curve (type-1 fuzzy) that describes the variables' degree of membership to a fuzzy set, using a value between 0 and 1. Membership functions are used in a fuzzification process to convert the crisp values to fuzzy values [25]. Membership functions can be implemented using a variety of functions, such as triangular, Gaussian, or gamma. Here, we chose the Gaussian membership function due to the similarity of this function with many biological processes. In general, Gaussian membership functions are popular because of their smoothness and concise notation [26]. MFs designed with Gaussian forms are modified by tuning the standard deviation and their mean values, as shown in Table 2. Table 1 indicates the fact that low mineralization volume and close data points in a 7-day culturing period compared to the 14- and 21-day periods results in a smaller standard deviation than the two other MFs.

Table 1. Input Bioprinting data.

Culture Period (Days)	Cell Suspension Density (Million Cells /Milliliter)	Mineralization Volume (mm ³)
7	0	0
7	1.67	0.1
7	5	0.1
7	15	0.2
14	0	0
14	1.67	1
14	5	3
14	15	12
21	0	4
21	1.67	14
21	5	21
21	15	24

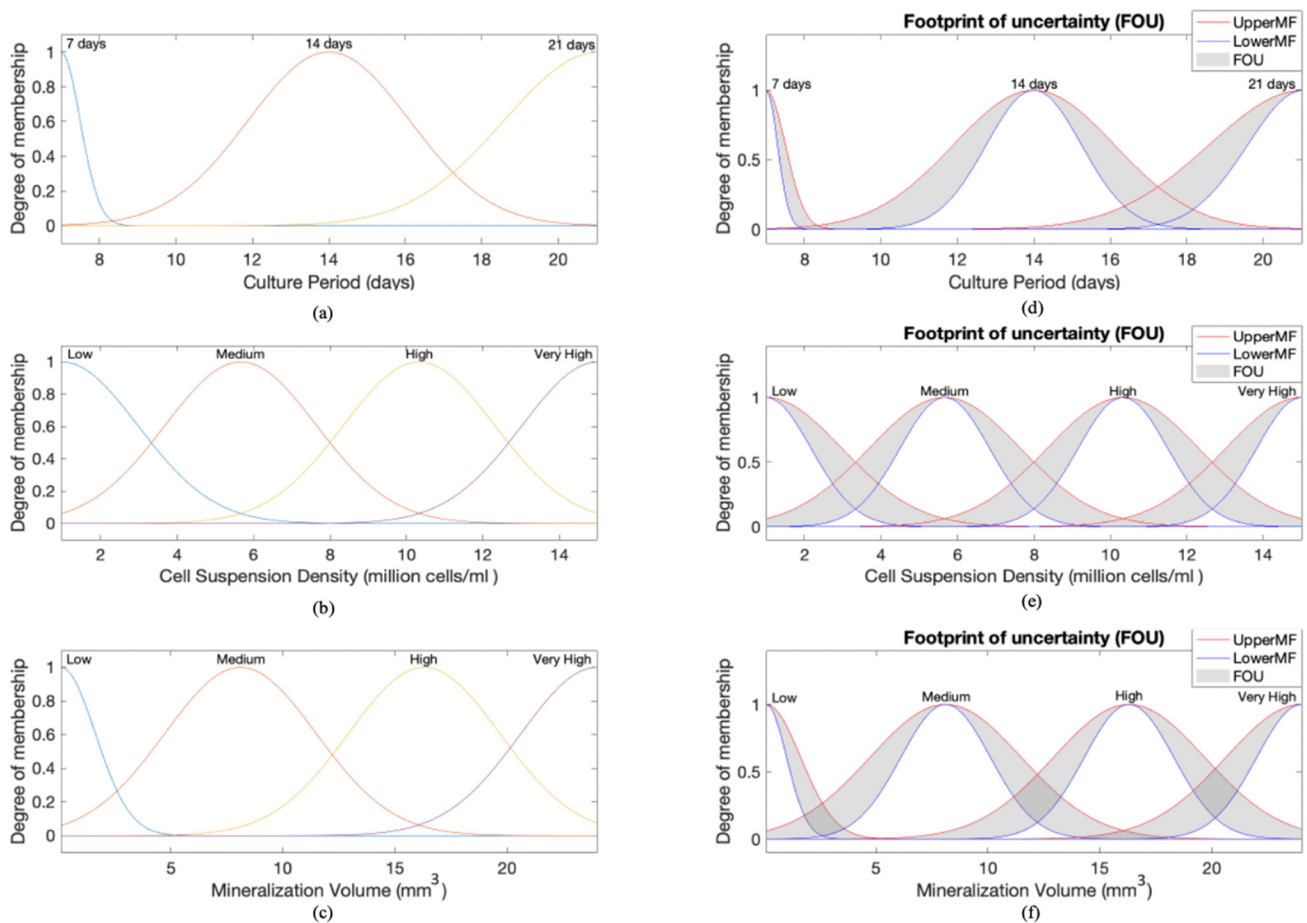


Figure 3. Type-1 and Type-2 Fuzzy Membership Functions. (a–c) Type-1 MFs for the two inputs, (a) culture period and (b) cell suspension density, as well as the single output (c) mineralization volume. (d–f) Type-2 MFs for (d) culture period, (e) cell suspension density, and (f) mineralization volume. Type-2 membership functions are designed with 0.2 lag. Upper (red) and lower (blue) boundaries are as illustrated.

Table 2. Gaussian membership functions range [Sigma, Mean].

Linguistic Variable	Culture Period (Days)	Cell Suspension Density (Million Cells /Milliliter)	Mineralization Volume (mm ³)
Low	[0.5011 6.78]	[1.981 1]	[1.54 0.1]
Medium	[2.109 14]	[1.981 5.667]	[3.38 8.11]
High	[2.476 21.03]	[1.981 10.33]	[3.384 16.03]
Very High	-	[1.981 15]	[3.384 24]

The membership functions based on the input value representation (Table 1) are plotted in Figure 3. The Type-1 membership functions were converted to Type-2 with a prescribed 20 and 30 percent uncertainty using the Fuzzy Logic System toolbox (Matlab). The lower and upper boundary of the MFs type-2 FS with 0.2 lag are plotted in Figure 3.

2.3. If-Then Rules Establishment

The next step in designing a fuzzy system is to define the fuzzy IF-THEN rules. As shown in Table 2, we utilized previously published results from an experimental bioprinting study [23]. The model rules are shown in Table 3.

Table 3. Type-1 and Type-2 Fuzzy system rules.

Rule	Culture Period (Days)	Cell Suspension Density (Million Cells/Milliliter)	Mineralization Volume (mm ³)
1	Low	Low	Low
2	Low	Medium	Low
3	Low	High	Low
4	Low	Very High	Low
5	Medium	Low	Low
6	Medium	Medium	Medium
7	Medium	High	Medium
8	Medium	Very High	High
9	High	Low	Medium
10	High	Medium	High
11	High	High	Very High
12	High	Very High	Very High

2.4. Fuzzy Inference Process

Finally, we implemented the type-1 fuzzy inference process using the following procedure:

1. Fuzzification of the input variables;
2. Application of the fuzzy operator (AND) in the antecedent;
3. Implication from the antecedent to the consequent;
4. Aggregation of the consequent across the rules;
5. Defuzzification.

Next, the type-2 fuzzy system is implemented using the following process:

1. Fuzzification of the input variables;
2. Application of the fuzzy operator (AND) in the antecedent;
3. Convert T1 MF to T2 MF with 0.2 and 0.3 lag;
4. Implication from the antecedent to the consequent;
5. Aggregation of the consequent across the rules;
6. T2 FS to T1 FS type reduction by Karnik–Mendel;
7. Defuzzification.

In the above process, we use “Minimum” for AND (Step 2), “Minimum” for Implication (Step 4), “Maximum” for Aggregation (Step 5), and “Centroid” for defuzzification (Step 7). We used the “Centroid” defuzzification because it has the highest correlation in defuzzification methods in comparison to the other methods, such as bisector, mean of maximum, and largest of maximum for non-interval data, as previously described [22]. The 3D surface of the implemented type-1 fuzzy and type-2 fuzzy (20% and 30% uncertainty) rules based on the two inputs and one output is plotted in Figure 4.

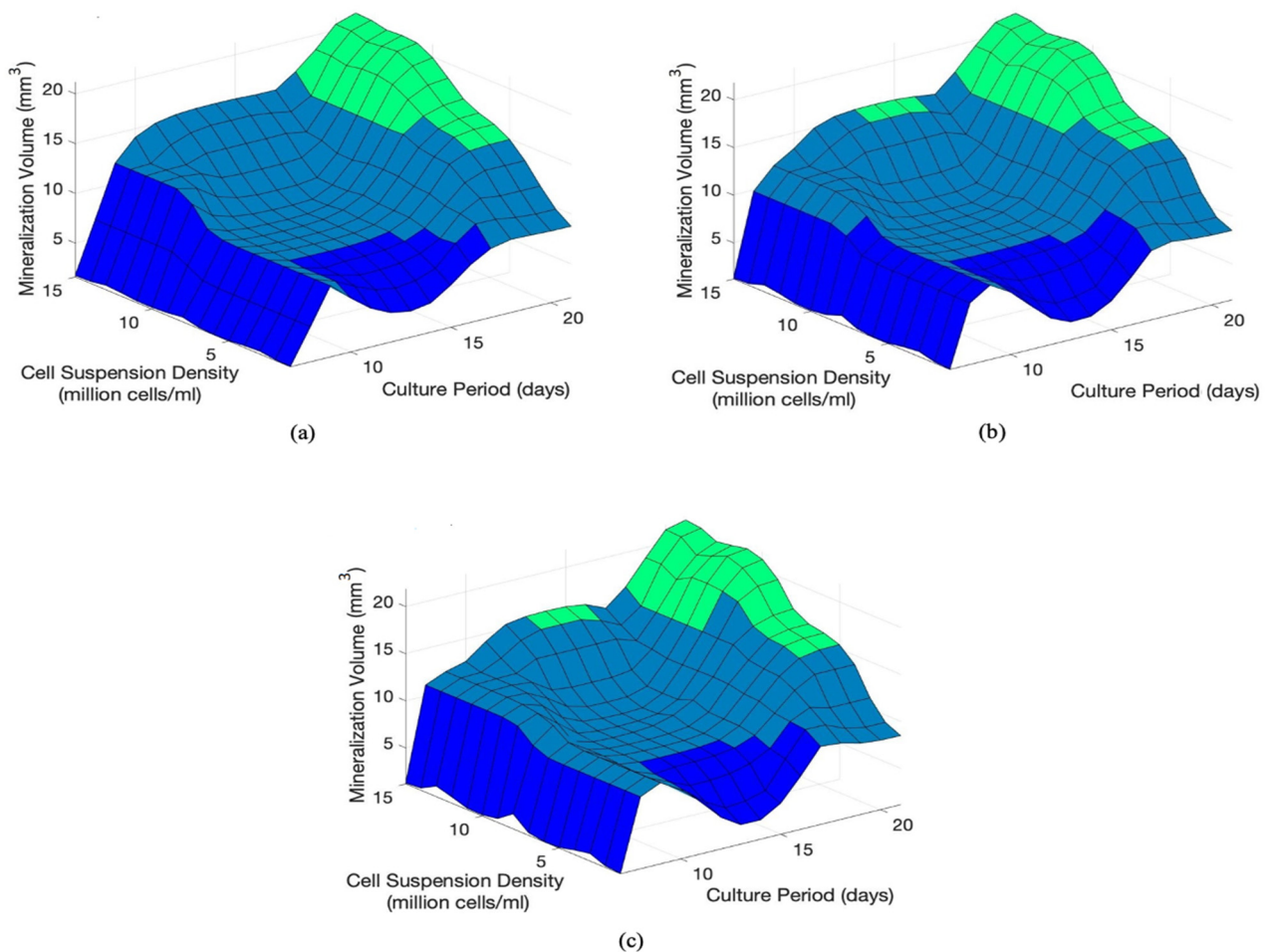


Figure 4. 3D surfaces generated by implemented fuzzy rules. (a) Type-1 fuzzy system. (b) Type-2 fuzzy system with 20% uncertainty. (c) Type-2 fuzzy system with 30% uncertainty.

3. Results

Type-1 and type-2 fuzzy systems were implemented as described using input data from a previous experimental study [23]. Table 4 shows the T1 and T2 FS approximated values. In these tables, in addition to the experimental input data, the type-2 fuzzy model has an additional input, which is the uncertainty boundary (either 20% or 30%). This uncertainty boundary is used as an input to compare the mineralization volume output with different noise levels in the input data.

First, we generated approximated values at each of the input value combinations available (Table 4). A graphical visualization of these values has been generated as a 3D surface, for the T1 FS (Figure 4a), 20% T2 FS (Figure 4b), and 30% T2 FS (Figure 4c). Next, we compared the experimental output value (mineralization volume) to the approximated values in each of the three fuzzy systems (Table 4). Here, we calculated the root mean square error (RMSE) between the experimental and approximated values with the same input values.

The equation of the measurement is given as follows (8):

$$RMSE = \sqrt{\frac{\sum_{i=1}^N (x_i - \bar{x}_i)^2}{N}} \quad (8)$$

Compared to the T1 FS, we observed that the 20% T2 FS increases the overall error of the approximation (+5.3%). In contrast, we observed that the 30% T2 FS decreases the overall error of the approximation (−2.8%), relative to the T1 FS.

Table 4. Accuracy of Type-1 and Type-2 (20% and 30% uncertainty) Fuzzy Systems.

Culture Period (Days)	Cell Suspension Density (Million Cells /Milliliter)	Mineralization Volume (mm ³)			
		Experimental Values (Actual)	Zero Uncertainty (T1 FS)	20% Uncertainty (T2 FS)	30% Uncertainty (T2 FS)
7	1.67	0.1	1.84	1.32	1.2
7	5	0.1	2.04	2.1	2.73
7	15	0.2	1.75	1.32	1.31
14	1.67	1	7.6	5.8	4.0
14	5	3	8.28	8.21	8.21
14	15	12	15.57	15.58	15.87
21	1.67	14	9.43	8.89	8.9
21	5	21	14.9	15.4	15.45
21	15	24	21.2	21.81	21.89
	RMSE	N/A	3.6	3.79	3.5

4. Discussion

Bioprinting research is a time-consuming and expensive process requiring the use of cells that may be difficult to source followed by a lengthy culture period. Finally, quantification of the suitability of the bioprint itself can be challenging. As a result, it is difficult to exhaustively optimize a bioprinted construct experimentally. Here, we have demonstrated that approximating bioprinting output parameters using fuzzy systems based on input variables is a viable approach to accelerate research, reduce experimental costs, and improve outcomes. Furthermore, our fuzzy model approach can be redesigned with additional input and output variables, qualitative results, or expert knowledge using linguistic rules.

In this study, we implement a fuzzy logic-based model using both type-1 and type-2 fuzzy systems to compare the results in handling the uncertainty associated with the bioprinting process. This uncertainty can arise from noisy input data or imperfect expert knowledge. Using experimental data, we have demonstrated that the implemented fuzzy logic can convert the discrete crisp input data to fuzzy sets to achieve a continuum data surface with high accuracy.

Additional work may be necessary to determine the specific level of uncertainty necessary to achieve the highest accuracy. Moreover, further experimental work is required to scrutinize the accuracy of this model. Nonetheless, since the increased range of uncertainty may increase the overfitting variance, we used 30% percent uncertainty level as the highest boundary to alleviate the bias–variance tradeoff [27]. In this experiment, the results with two different uncertainty percentages indicate a high correlation with experimental data. Furthermore, the 30% type-2 fuzzy model can accommodate more imprecision with higher accuracy. In contrast, the 20% type-2 fuzzy model could not provide higher accuracy relative to the type-1 fuzzy model.

We have provided 3D surfaces generated by the fuzzy rules (e.g., Figure 4) as an intuitive tool to help researchers design new studies for the experimental optimization of bioprinted constructs. For example, researchers should avoid performing new experiments in “flat” areas of the 3D model. In our study, the 3D surface illustrates a relatively flat area for moderate cell suspension densities and culture periods of around 14 days. Therefore, if a researcher wishes to maximize mineralization volume with a low number of cells (e.g., 5×10^6 cells/mL), they may prefer to increase their culture time to 21 days rather

than attempt to triple their cell number in order to traverse the flat area of the surface. In total, implementation of this system may help researchers optimize their study design to eliminate unnecessary experimentation.

We also note that the 3D surfaces generated for the type-2 fuzzy models (Figure 4b,c) are both qualitatively smoother than the surface generated using the type-1 fuzzy system (Figure 4a). In particular, we observe a sharp edge around a culture period of 8 days (Figure 4a). This smoothness in Figure 4b,c is likely to result in higher accuracy in approximated values, as biological mathematical models ought to have a smooth transmission when increasing the input values.

Author Contributions: Conceptualization, A.S. and R.E.T.; methodology, A.S. and M.-R.A.-T.; software, A.S.; validation, A.S. and M.-R.A.-T.; formal analysis, R.E.T.; investigation, M.-R.A.-T.; resources, A.S. and R.E.T.; data curation, A.S. and R.E.T.; writing—original draft preparation, A.S. and R.E.T.; writing—review and editing, R.E.T. and M.-R.A.-T.; visualization, A.S.; supervision, R.E.T.; project administration, R.E.T.; funding acquisition, R.E.T. All authors have read and agreed to the published version of the manuscript.

Funding: This study received no external funding.

Data Availability Statement: The experimental data referenced in this study have been previously published [23].

Acknowledgments: Research in the Tomlinson lab is supported by the National Institute of Arthritis and Musculoskeletal and Skin Diseases and the National Institute of Dental and Craniofacial Research of the National Institutes of Health under award numbers AR074953 (RET) and DE028397 (RET). The content is solely the responsibility of the authors and does not necessarily represent the official views of the funding bodies.

Conflicts of Interest: The authors declare no conflict of interest.

References

1. Sedigh, A.; Kachooei, A.R.; Beredjikian, P.K.; Vaccaro, A.R.; Rivlin, M. Safety and Efficacy of Casting During COVID-19 Pandemic: A Comparison of the Mechanical Properties of Polymers Used for 3D Printing to Conventional Materials Used for the Generation of Orthopaedic Orthoses. *Arch. Bone Jt. Surg.* **2020**, *8*, 281–285. [[CrossRef](#)] [[PubMed](#)]
2. Sedigh, A.; Ebrahimzadeh, M.H.; Zohoori, M.; Kachooei, A. Cubitus Varus Corrective Osteotomy and Graft Fashioning Using Computer Simulated Bone Reconstruction and Custom-Made Cutting Guides. *Arch. Bone Jt. Surg.* **2020**, *9*, 467–471. [[CrossRef](#)]
3. Derakhshanfar, S.; Mbeleck, R.; Xu, K.; Zhang, X.; Zhong, W.; Xing, M. 3D bioprinting for biomedical devices and tissue engineering: A review of recent trends and advances. *Bioact. Mater.* **2018**, *3*, 144–156. [[CrossRef](#)]
4. Murphy, S.V.; Atala, A. 3D bioprinting of tissues and organs. *Nat. Biotechnol.* **2014**, *32*, 773–785. [[CrossRef](#)] [[PubMed](#)]
5. Koo, T.K.; Li, M.Y. A Guideline of Selecting and Reporting Intraclass Correlation Coefficients for Reliability Research. *J. Chiropr. Med.* **2016**, *15*, 155–163. [[CrossRef](#)]
6. Webb, B.; Doyle, B. Parameter optimization for 3D bioprinting of hydrogels. *Bioprinting* **2017**, *8*, 8–12. [[CrossRef](#)]
7. Sedigh, A.; Tulipan, J.E.; Rivlin, M.R.; Tomlinson, R.E. Utilizing Q-Learning to Generate 3D Vascular Networks for Bioprinting Bone. *bioRxiv* **2020**. [[CrossRef](#)]
8. Suntornnond, R.; Tan, E.Y.S.; An, J.; Chua, C.K. A Mathematical Model on the Resolution of Extrusion Bioprinting for the Development of New Bioinks. *Materials* **2016**, *9*, 756. [[CrossRef](#)]
9. Sedigh, A.; DiPiero, D.; Shine, K.M.; Tomlinson, R.E. Enhancing precision in bioprinting utilizing fuzzy systems. *Bioprinting* **2022**, *25*, e00190. [[CrossRef](#)]
10. Sedigh, A.; Ghelich, P.; Quint, J.; Samandari, M.; Tamayol, A.; Tomlinson, R.E. Approximating Scaffold Printability Utilizing Computational Methods. *bioRxiv* **2022**. [[CrossRef](#)]
11. Torres, A.; Nieto, J.J. Fuzzy Logic in Medicine and Bioinformatics. *J. Biomed. Biotechnol.* **2006**, *2006*, 091908. [[CrossRef](#)] [[PubMed](#)]
12. Olofsson, S.; Mehrian, M.; Calandra, R.; Geris, L.; Deisenroth, M.P.; Misener, R. Bayesian Multiobjective Optimisation With Mixed Analytical and Black-Box Functions: Application to Tissue Engineering. *IEEE Trans. Biomed. Eng.* **2018**, *66*, 727–739. [[CrossRef](#)] [[PubMed](#)]
13. Göhl, J.; Markstedt, K.; Mark, A.; Håkansson, K.M.O.; Gatenholm, P.; Edelvik, F. Simulations of 3D bioprinting: Predicting bioprintability of nanofibrillar inks. *Biofabrication* **2018**, *10*, 034105. [[CrossRef](#)]
14. Bordon, J.; Moskon, M.; Zimic, N.; Mraz, M. Fuzzy Logic as a Computational Tool for Quantitative Modelling of Biological Systems with Uncertain Kinetic Data. *IEEE/ACM Trans. Comput. Biol. Bioinform.* **2015**, *12*, 1199–1205. [[CrossRef](#)] [[PubMed](#)]
15. Luo, Z.-P.; Zhang, L.; Turner, R.; An, K.-N. Effects of mechanical stress/strain and estrogen on cancellous bone structure predicted by fuzzy decision. *IEEE Trans. Biomed. Eng.* **2000**, *47*, 344–351. [[CrossRef](#)]

16. Baghbani, F.; Akbarzadeh-T., M.-R.; Akbarzadeh, A. Indirect adaptive robust mixed H_2/H_∞ general type-2 fuzzy control of uncertain nonlinear systems. *Appl. Soft Comput.* **2018**, *72*, 392–418. [[CrossRef](#)]
17. Toloue, S.F.; Akbarzadeh, M.-R.; Akbarzadeh, A.; Jalaieian-F, M. Position tracking of a 3-PSP parallel robot using dynamic growing interval type-2 fuzzy neural control. *Appl. Soft Comput.* **2015**, *37*, 1–14. [[CrossRef](#)]
18. Hassanzadeh, H.R.; Akbarzadeh-T., M.-R.; Akbarzadeh, A.; Rezaei, A. An interval-valued fuzzy controller for complex dynamical systems with application to a 3-PSP parallel robot. *Fuzzy Sets Syst.* **2014**, *235*, 83–100. [[CrossRef](#)]
19. Mendel, J.M. A comparison of three approaches for estimating (synthesizing) an interval type-2 fuzzy set model of a linguistic term for computing with words. *Granul. Comput.* **2015**, *1*, 59–69. [[CrossRef](#)]
20. Karnik, N.; Mendel, J.; Liang, Q. Type-2 fuzzy logic systems. *IEEE Trans. Fuzzy Syst.* **1999**, *7*, 643–658. [[CrossRef](#)]
21. Melin, P.; Castillo, O. A review on type-2 fuzzy logic applications in clustering, classification and pattern recognition. *Appl. Soft Comput.* **2014**, *21*, 568–577. [[CrossRef](#)]
22. Mogharreban, N.; DiLalla, L.F. Comparison of Defuzzification Techniques for Analysis of Non-interval Data. In Proceedings of the NAFIPS 2006—2006 Annual Meeting of the North American Fuzzy Information Processing Society, Montreal, QC, Canada, 3–6 June 2006; pp. 257–260. [[CrossRef](#)]
23. Zhang, J.; Wehrle, E.; Adamek, P.; Paul, G.R.; Qin, X.-H.; Rubert, M.; Müller, R. Optimization of mechanical stiffness and cell density of 3D bioprinted cell-laden scaffolds improves extracellular matrix mineralization and cellular organization for bone tissue engineering. *Acta Biomater.* **2020**, *114*, 307–322. [[CrossRef](#)] [[PubMed](#)]
24. Vetsch, J.R.; Müller, R.; Hofmann, S. The influence of curvature on three-dimensional mineralized matrix formation under static and perfused conditions: An *in vitro* bioreactor model. *J. R. Soc. Interface* **2016**, *13*, 20160425. [[CrossRef](#)]
25. Moreno-Cabezali, B.M.; Fernandez-Crehuet, J.M. Application of a fuzzy-logic based model for risk assessment in additive manufacturing R&D projects. *Comput. Ind. Eng.* **2020**, *145*, 106529. [[CrossRef](#)]
26. Sadollah, A. Introductory Chapter: Which Membership Function is Appropriate in Fuzzy System? In *Fuzzy Logic Based in Optimization Methods and Control Systems and its Applications*; InTech: Singapore, 2018. [[CrossRef](#)]
27. Ge, D.; Zeng, X.-J. Learning data streams online—An evolving fuzzy system approach with self-learning/adaptive thresholds. *Inf. Sci.* **2019**, *507*, 172–184. [[CrossRef](#)]